Numerical Examples of Compact Constant Mean Curvature Surfaces

Karsten Große-Brauckmann Konrad Polthier

December 15, 1994

Abstract

We construct new examples of compact CMC surfaces of higher genus numerically. A conjugate surface method allows to explicitly construct examples. We employ the numerical algorithm of Oberknapp and Polthier based on discrete techniques to find area minimizers in the sphere $\mathbb{S}^3$ and to conjugate them to surfaces of constant mean curvature in $\mathbb{R}^3$. We compute examples of genus 5 and 12 and discuss a further example of genus 3.

Contents

1 Introduction

For a long time the sphere has been the only known compact immersed surface of constant mean curvature (CMC). By the result of Alexandrov there is no other embedded compact CMC surface and by a theorem of Hopf the only way to immerse the sphere with CMC is the round sphere. Nevertheless Wente discovered CMC tori in 1986 [W] (see Figure 2 and 3) and his work became the starting point for an intensive study of CMC surfaces.

Pinkall and Sterling classified all tori [PS] by the genus of a hyperelliptic curve and Bobenko then found explicit formulas in terms of theta functions [Bo, Thm.6.1]. These two papers actually consider a larger class of CMC surfaces containing the tori. Algebraic conditions for the solvability of the period problem were stated in [Bo], and Ercolani, Knörrer, Trubowitz [EKT] (also Jaggi [J]) proved that for hyperelliptic curves of each genus these conditions are satisfied. Hence there are CMC tori for every genus. Heil has evaluated Bobenko's formulas numerically and is in a position to decide on the existence of the tori [H].

Kapouleas constructed compact CMC surfaces of every genus greater than two by an implicit function argument [Kp1]. Each surface is based on a graph such that the vertices relate to spheres and the edges to pieces of Delaunay surfaces. Provided the graph is balanced, Kapouleas proves there exists a surface for a suitable scaling of the graph. This means that the edges contain a possibly big number of Delaunay 'bubbles', and – similar to the situation for tori – it is not known explicitly what these surfaces look like. In [Kp2] also surfaces of genus two are constructed by fusing two Wente tori together.

For the first time a conjugate surface method was used by Lawson 1970 [L] to prove existence of CMC surfaces and later extended by Karcher [Ka] and one of the authors [G-B1]. They constructed a number of periodic CMC surfaces and surfaces with ends, as well as the Wente torus [G-B2]. The conjugate surface method is more explicit than Kapouleas' method and works for sufficiently symmetric surfaces.

In the present work we use this method to construct numerically new compact CMC surfaces of higher genus. As candidates we take highly symmetric CMC surfaces 'close' to a collection of spheres which are joint by small handles. Existence of the Penta surface of genus 5 and the surface with dodecahedral symmetry of genus 12 is discussed in detail, while the numerics could not decide an example of genus 3. With any of the methods mentioned before a hard problem is to solve the period problem. In simpler cases it can be settled by an intermediate value theorem [Ka] using a graph property, or by a degree argument [G-B2].

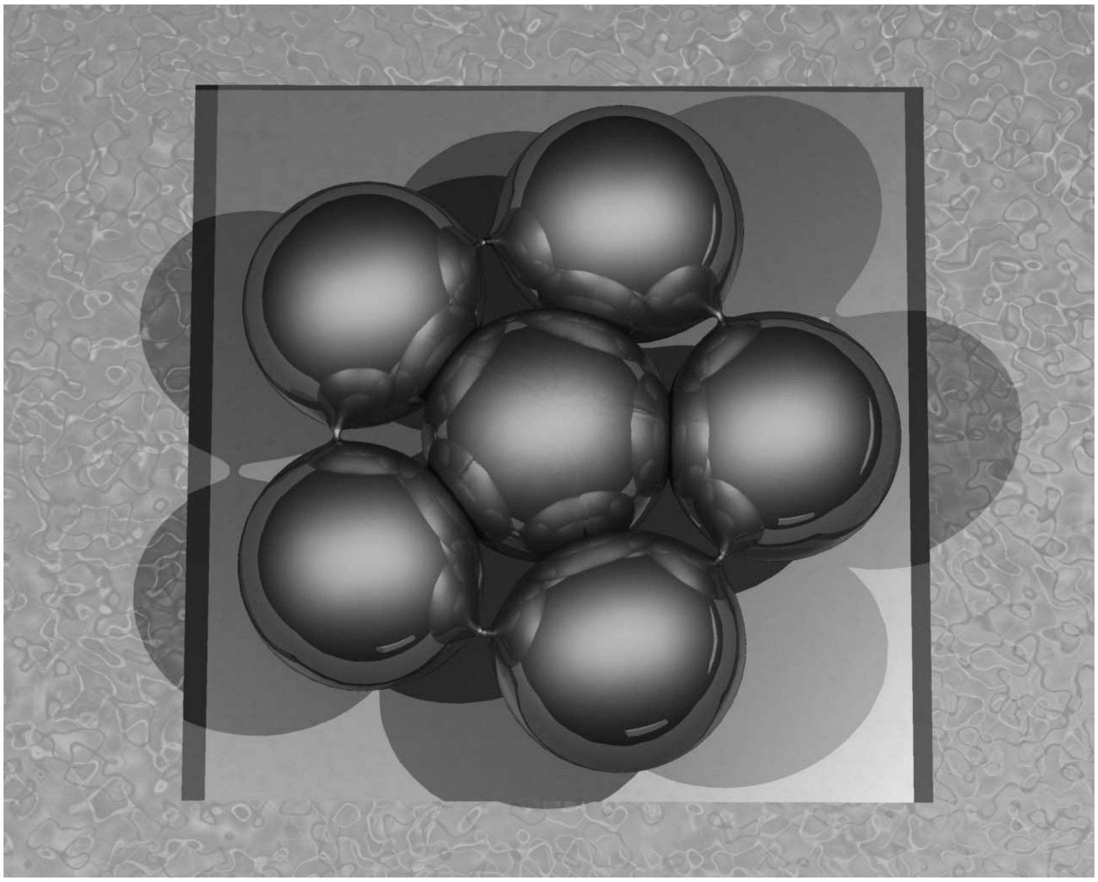

Figure 1: Surface Penta of genus 5. Small unduloidal handles connect the five outer spheres which, in turn, are joined to a centre sphere with nodoidal handles.

Here we use the numerical algorithm of Oberknapp and Polthier [O] [OP] to deal with the period problem in more involved situations. The algorithm uses discrete techniques generalizing an algorithm of Pinkall and Polthier [PP] for minimal surfaces.

At first we review in Section 2 the conjugate surface construction for CMC surfaces, in its standard C^2 description as well as in the C^1 form that is used for the numerical algorithm. We also explain the period problem that makes our examples unique (or isolated) for fixed symmetries. We then review the underlying discrete numerical algorithm in Section 3. In Section 4 we discuss a class of possible candidates, where the necessary conditions of stability and balancing are satisfied. Three specific examples and their numerics are described in Section 5 in greater detail.

The algorithms and the graphics were implemented using the mathematical

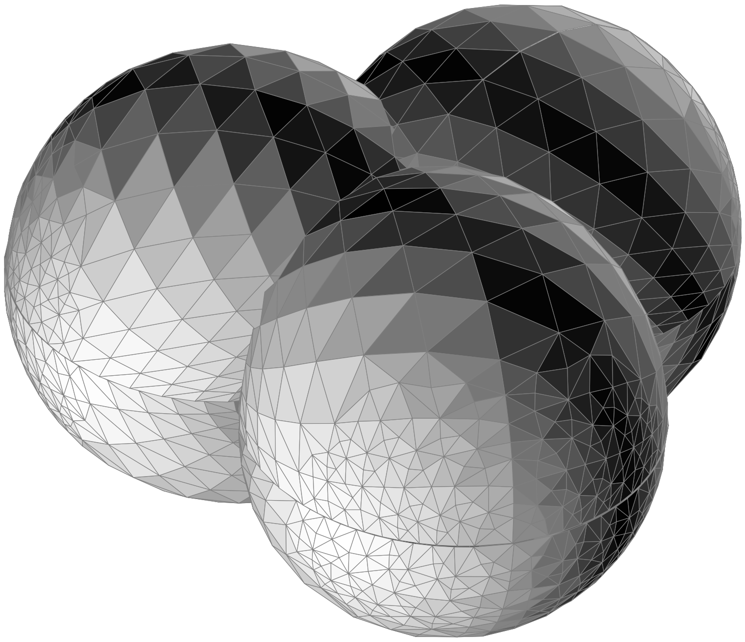

Figure 2: Wente torus with three lobes

programming environment Grape developed at the Sonderforschungsbereich 256 at the University of Bonn. Grape can be obtained on request via the second author.

2 The conjugate surface construction

We illustrate the main ideas of this method. For details see [G-B1].

It is helpful to explain the conjugate surface construction for minimal surfaces in $\mathbb{R}^3$ first. Let F be an immersion with normal N, metric $g(v,w) = dF(v) \cdot dF(w)$ and Weingarten map A given by $g(Av,w) = dN(v) \cdot dF(w)$. A surface is determined by its metric g and Weingarten map A provided the integrability conditions, the equations of Gauß and Codazzi, are satisfied.

For a simply connected piece of an oriented minimal surface M there is another surface $\tilde{M}$, the *conjugate surface*, with geometric data $\tilde{g}, \tilde{A}$ given by

$$\tilde{g} = g \quad \text{and} \quad \tilde{A} = R^{\pi/2} \circ A, \tag{1}$$

where $R^{\pm\pi/2}$ denotes rotation by $\pm\pi/2$ with respect to the metric g. The integrability conditions for M can be checked to imply those of $\tilde{M}$.

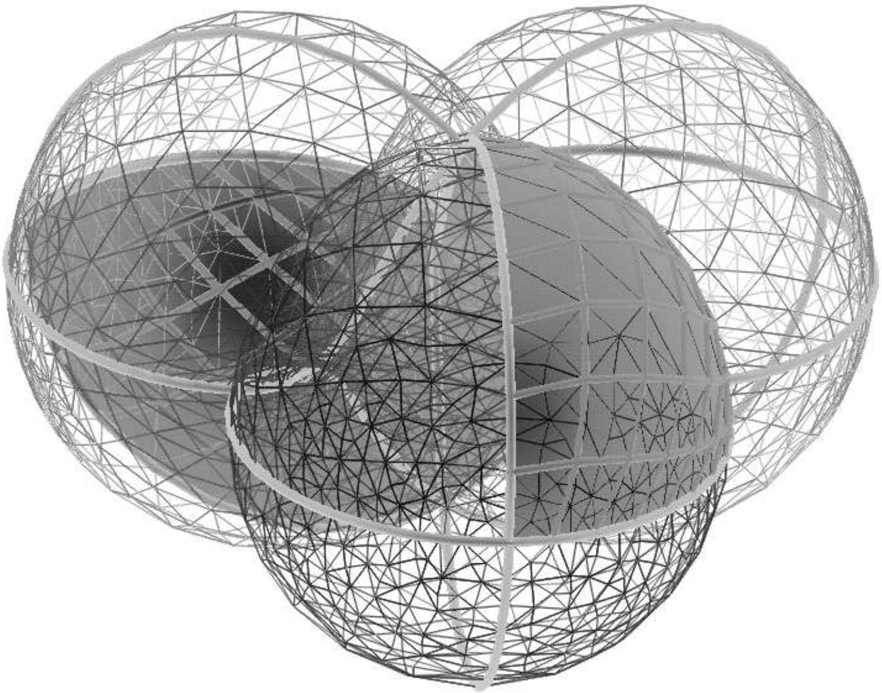

Figure 3: A grid model of the same Wente torus. A fundamental domain that generates the surface by planar reflection is highlighted.

Suppose we have an idea for the shape of a minimal surface with planar symmetries, and the surface modulo its symmetries gives a simply connected compact *fundamental patch.* To prove existence of such a patch via the conjugate surface construction it is essential that conjugation interchanges curvature and asymptote lines, and that geodesics are preserved. This is useful since the fundamental patch is bounded by planar, i.e. geodesic curvature lines, and hence relates to a conjugate patch bounded by geodesic asymptote lines. These lines are geodesics of the ambient space $\mathbb{R}^3$, i.e. straight lines, and therefore the conjugate patch is bounded by a polygon which has only finitely many parameters. We prove the claimed property in case $F(x)$ is a conformal curvature line parameterization of $\tilde{M}$. Let us write A in matrix form, $A\frac{\partial}{\partial x_i} = A_i^j \frac{\partial}{\partial x_j}$. According to (1)

$$(2)\quad \tilde{A} = \begin{pmatrix} -\kappa & 0 \\ 0 & \kappa \end{pmatrix} \quad \text{and} \quad A = R^{-\pi/2}\tilde{A} = \begin{pmatrix} 0 & 1 \\ -1 & 0 \end{pmatrix} \begin{pmatrix} -\kappa & 0 \\ 0 & \kappa \end{pmatrix} = \begin{pmatrix} 0 & \kappa \\ \kappa & 0 \end{pmatrix}$$

i.e. the parametrization of M is in asymptote lines.

We now want to determine the polygon on M from the fundamental patch on $\tilde{M}$. Let the polygon on $\tilde{M}$ be bounded by n planar curvature arcs $\tilde{\gamma}_i$. Then the conjugate arcs make the same angles at the vertices on the isometric surface M.

Moreover, by definition of A we obtain quantitative information from (2): The turning speed $-\kappa$ of the normal along the planar curvature line $\tilde{\gamma}_i$ on $\tilde{M}$ equals the rotation speed κ of the normal along the straight line γ_i of M. In particular, by an integration of (2) the total turn $\tilde{\tau}_i$ of the normal along the planar curvature line $\tilde{\gamma}_i$ equals the total rotation ρ_i of the normal along the straight arc γ_i,

$$-\tilde{\tau}_i = \rho_i.$$

A closed polygon of straight arcs on M is not completely determined by the n vertex angles and the n total rotations ρ_i (up to Euclidean motions and scaling); in general we are free to specify $n-3$ lengths of the polygon. For a given patch bounded by planar symmetry curves this gives an $n-3$ parameter family of closed polygonal candidates. Hence by taking solutions to Plateau's problem for each closed polygon we get an $n-3$ parameter family of minimal patches M. Each conjugate patch $\tilde{M}$ can be reflected by the assumed group of planar symmetries to a complete branched immersed surface.

Lawson generalized this approach to CMC surfaces [L]. He found a one to one correspondence between CMC surfaces in $\mathbb{R}^3$ and minimal surfaces in S^3.

Theorem 1 *If M is a simply connected minimal surface in S^3 with data g, A, then there exists a CMC surface $\tilde{M} \subset \mathbb{R}^3$ with*

$$\tilde{g} = g \quad \textit{and} \quad \tilde{A} = \mathrm{id} + R^{\pi/2} \circ A. \tag{3}$$

In place of (2) we now have

$$A = \begin{pmatrix} 0 & \kappa \\ \kappa & 0 \end{pmatrix} \quad \text{and} \quad \tilde{A} = \mathrm{id} + R^{\pi/2} \circ A = \begin{pmatrix} 1-\kappa & 0 \\ 0 & 1+\kappa \end{pmatrix} \tag{4}$$

and this shows that $\tilde{M}$ is a CMC immersion.

We can make the same construction as in the minimal case, because $\gamma_i \subset \mathrm{S}^3$ is ambient geodesic, or a great circle arc, if and only if $\tilde{\gamma}_i \subset \mathbb{R}^3$ is a planar curvature arc. Again we integrate $1-\kappa$ resp. κ along the boundary arcs to the total turn $\tilde{\tau}_i$ of the normal along an arc $\tilde{\gamma}_i$ of the CMC patch and the total rotation ρ_i along the spherical arc γ_i of the respective minimal patch. This gives

$$|\gamma_i| - \tilde{\tau}_i = \rho_i \tag{5}$$

where $|\gamma_i|$ is the length of γ_i. Although the lengths in (5) make it more complicated we can find an $n-3$ parameter family of closed spherical polygons with great circle arcs as before. We take Morrey's solution M to the Plateau problem for such a polygon and conjugate back to a branched CMC surface $\tilde{M} \subset \mathbb{R}^3$.

We are usually interested in further properties of $\tilde{M}$. For instance if we rule out branch points at the vertices then the complete CMC surface turns out to be smooth. Moreover we want to specify τ_i as a real number; but both τ_i and τ_i plus integer multiples of 2π give rise to the same polygon. The standard way to deal with these problems is to embed the spherical boundary polygon into the boundary of a mean convex set.

2.1 A C^1-description of conjugation

The description explained before is disadvantageous for numerical considerations since a number of different numerical algorithms must be applied successively – all incorporating additional numerical inaccuracies: The spherical surface M is the result of an area minimization process, this surface has to be differentiated twice, and finally the obtained geometric data must be integrated to the CMC surface $\tilde{M}$. The discrete algorithm is based on a C^1 description which in the smooth case requires only one differentiation and integration. This description can be given for both minimal and CMC surfaces. For details see [OP].

For the minimal surface case let Ω be a Riemann surface and $F : \Omega \to \mathbb{R}^3$ be a minimal immersion of Ω with normal vector field N. Then the conjugate surface $\tilde{F} : \Omega \to \mathbb{R}^3$ is given by the differential system

$$\begin{aligned} d\tilde{F} &= dF \circ R^{\pi/2} \\ \tilde{N} &= N. \end{aligned}$$

In a similar way the conjugate CMC surfaces can be obtained from a spherical minimal surface. Take the Lie group representation of S^3 and identify S^3 with the unitary quaternions such that for $x \in \mathrm{S}^3$ we have $x = x_0 + x_1\mathbf{i} + x_2\mathbf{j} + x_3\mathbf{k}$. We identify $\mathbb{R}^3$ with the imaginary quaternions, $\operatorname{Im} x = (x_1, x_2, x_3)$. With $\bar{x} = x_0 - x_1\mathbf{i} - x_2\mathbf{j} - x_3\mathbf{k}$ the quaternion product is $\bar{x}y := (\langle x, y\rangle_{\mathbb{R}^4},\ x_0 \operatorname{Im} y - y_0 \operatorname{Im} x - \operatorname{Im} x \times \operatorname{Im} y)$.

Lemma 2 *Let $F : \Omega \to \mathrm{S}^3$ be a minimal immersion, then the solution $\tilde{F} : \Omega \to \mathbb{R}^3$ of the differential system*

$$\begin{aligned} d\tilde{F} &= \operatorname{Im}(F dF \cdot R^{\pi/2}) \\ \tilde{N} &= \operatorname{Im}(FN) \end{aligned}$$

is the conjugate CMC surface in $\mathbb{R}^3$.

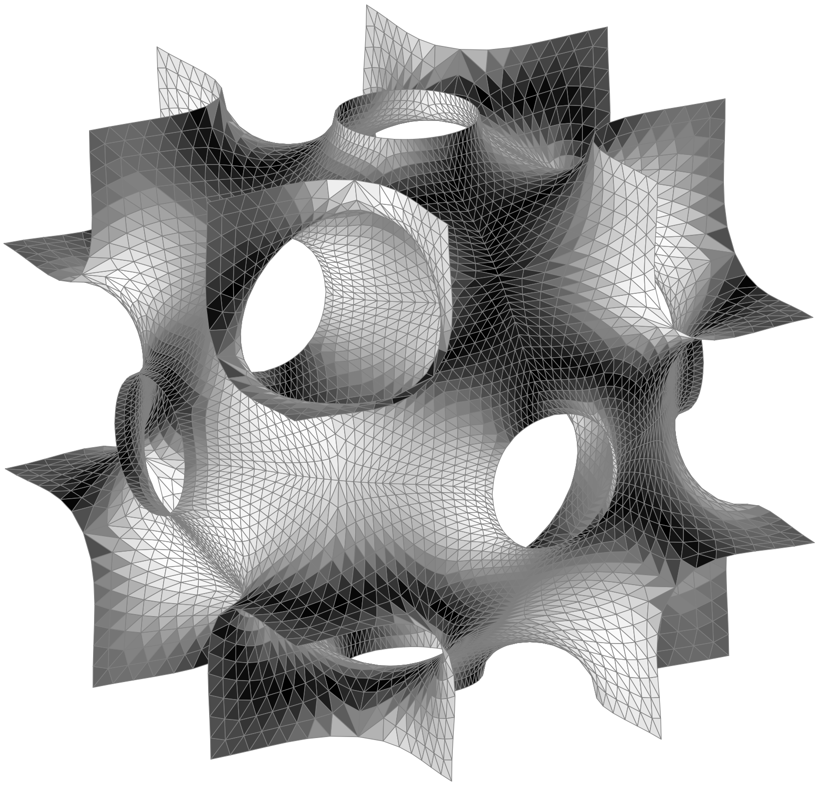

Figure 4: A translational fundamental domain of the triply periodic CMC surface O,C-TO (we use A. Schoen's notation for a similar minimal surface). The domain is inscribed in a cube and has all its symmetries. The handle considered in the next figure sits in the middle of each face of the cube.

2.2 The period problem

The period problem (compare Figures 4, 5) arises for compact CMC surfaces except for the sphere. Suppose we want two planar symmetry arcs of a fundamental CMC domain to be contained in the same plane. This is usually the case when an arc with total turn of the normal $\tilde{\tau}_i = \pm\pi$ is present. In general the $n-3$ parameter family of conjugate surfaces obtained from the spherical Plateau solutions leaves a nonzero translation, or *period*, between the two planes, and only a surface with a zero translation can generate a compact surface. If the periods can be closed at all, we expect that each period reduces the number of free parameters by one. The periods make our examples isolated (probably unique) in the class of surfaces we consider, i.e. with given symmetries: All examples in Section 5 have $n = 5$ boundary arcs and give rise to two period problems, whereas the Wente torus with $n = 4$ poses only one period problem.

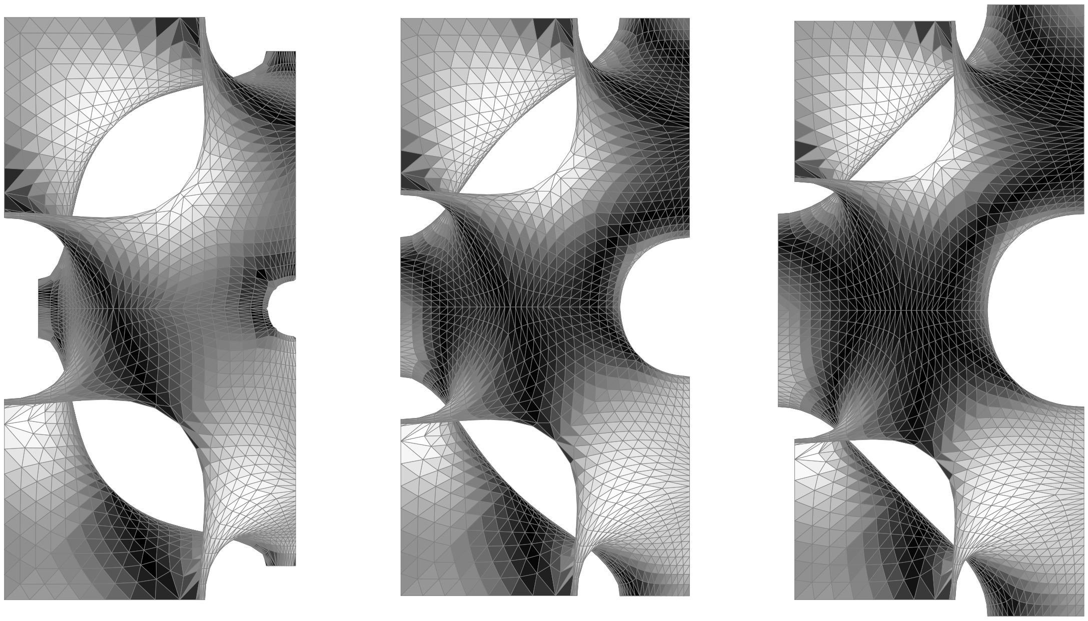

Figure 5: We demonstrate the period problem for O,C-TO. This surface can be generated by building an additional handle into the middle of each face of an I-WP CMC surface. This handle on the left side of the first image is too small (negative period, say), correctly sized in the second image (0 period), and too big (positive period) on the last image.

In the easiest case of a one-parameter family the period problem is solved by an intermediate value argument [Ka] [G-B2]: Two parameters with opposite periods are known, hence there is a surface with a vanishing period in between. Naturally, to apply the intermediate value theorem requires continuity of the surfaces in the parameter. This holds if the fundamental patch is graph, for instance for boundary curves that are themselves graph over a convex domain (see [Ka]). In [G-B2] a different argument is applied to the Wente torus; a continuous family is selected by a mapping degree argument.

3 Numerical algorithm for discrete CMC surfaces

Fundamental pieces of CMC surfaces are rarely stable if they are considered as a solution to a free boundary value problem. Hence a direct numerical approach to the minimization of area under a volume constraint works only under very restrictive hypotheses, for instance for graphs in tetrahedra, see Anderson [ADNS]. Alternatively, other integrals could be minimized, e.g. using Brakke's evolver [Br].

Unlike the previous approaches the algorithm of Oberknapp and Polthier uses the technique of discrete geometric surfaces and discrete descriptions of their properties. Before, this was applied by Pinkall and Polthier [PP] to compute minimal surfaces and their conjugates. The discrete technique does not try to approximate the smooth problem as it is for instance the goal of the finite element theory. Instead it reformulates the problem on a discrete level and uses a description which is exact on this level. The advantage of the discrete approach comes from the fact that one tries to approximate a smooth situation only once, namely in the last step when the discretization goes to zero.

Let us review the algorithm of Oberknapp and Polthier. For a detailed description we refer to [O] [OP]. The algorithm consists of two parts. The first part is a method to compute the Plateau solution as a discrete minimal surface in S^3. The second part consists of a conjugation procedure to compute the CMC surface in euclidean space from the above Plateau solution. Before sketching the minimization part let us clarify some terms:

Definition 3 (i) A *discrete surface in* S^3 is a simplicial complex in $\mathbb{R}^4$ consisting of triangles whose vertices are restricted to $S^3 \subset \mathbb{R}^4$; the triangles may degenerate to line segments or points. The surface is *discrete minimal* if variations of vertices constrained to S^3 do not decrease the area of the simplicial complex in $\mathbb{R}^4$.
(ii) If two discrete surfaces M_1, M_2 have the same abstract triangulation then a *simplicial map* $f : M_1 \to M_2$ maps the corresponding vertices onto each other and is linear on each triangle.

For a simplicial map we define the Dirichlet energy by

$$E(f) = \frac{1}{2}\int_M |\nabla f|^2 = \frac{1}{4}\sum_{\text{edges } a_i} (\cot \alpha_i + \cot \beta_i)\, |a_i|^2 ,$$

where $|a_i|$ denotes the length of the edge on the image surface and α_i, β_i are the angles opposite to the edge a_i in the two triangles containing a_i in the domain. Starting with a discrete initial surface M_0 we define inductively simplicial surfaces M_{k+1} to be the images of the minimum energy maps $f : M_k \to X$, where X runs through all simplicial complexes with the correct boundary conditions. It can be shown that the sequence M_k converges to a discrete minimal surface provided no triangles degenerate.

In a minimum M the following equation is satisfied at every vertex p of the triangulation

$$\frac{\partial}{\partial p}E(\mathrm{id})|_p = \frac{1}{2} \sum_{\substack{\text{vertices } q_i \\ \text{adjacent to } p}} (\cot\alpha_i + \cot\beta_i)(p - q_i)^{\tan_p} = 0 \tag{6}$$

Here $\tan_p : T_p\mathbb{R}^4 \to T_p\mathrm{S}^3$ gives the tangential part of the vector $p - q_i$. This allows the discrete definition of conjugation. Geometrically (6) means that the weighted tangential parts of the edges emanating from p in M add up to zero. Hence they can be arranged as a closed polygon in the tangent space. This polygon is defined to be the dual cell at the point p and can be understood as the integration of $*dF := dF \circ R^{\pi/2}$. Left translation moves the dual cell to the identity $T_{\mathrm{id}}\mathrm{S}^3$, where all cells are then reassembled (i.e. integration of the discrete data takes place) to a discrete CMC surface in $\mathbb{R}^3$. If we take an M_k, $k \neq 0$, in place of the minimum, conjugation is defined as above and the CMC surface is approximated.

The complete numerical algorithm consists of the following steps:

- Read vertex angles and the total turning angles $\tilde{\tau}_i$ of the normal vector along each edge γ_i of the fundamental patch for a euclidean CMC candidate. Guess edge lengths l_i. Fix $n-3$ lengths and take the remaining three lengths as an initial condition for a rootfinder. By an adjustment of these three lengths the rootfinder generates a polygonal contour Γ in S^3 with the given vertex angles and rotation of normal equal to $\rho_i = l_i - \tilde{\tau}_i$.

- Solve the Plateau problem for Γ. In our examples the Gauß curvature varies considerably within a patch. Therefore interactive local refinement of the triangulation in regions of high curvature is necessary.

- The conjugation algorithm transforms a discrete minimal surface in S^3 into a euclidean CMC surface.

- Check periods of the resulting CMC surface and repeat all steps with a different set of $n-3$ fixed initial lengths.

In practice we apply the algorithm to a one-parameter family of lengths at a time.

In principle, degeneracies can occur: The length of an edge can degenerate to 0 and also different arcs of the contour can intersect and give rise to two non-connected minimal patches which do not fulfill the original specification. Since the trigonometric formulae for the edge lengths are involved we use a numerical algorithm, a rootfinder, to compute the exact values. In practise we are 'far away' from these degeneracies.

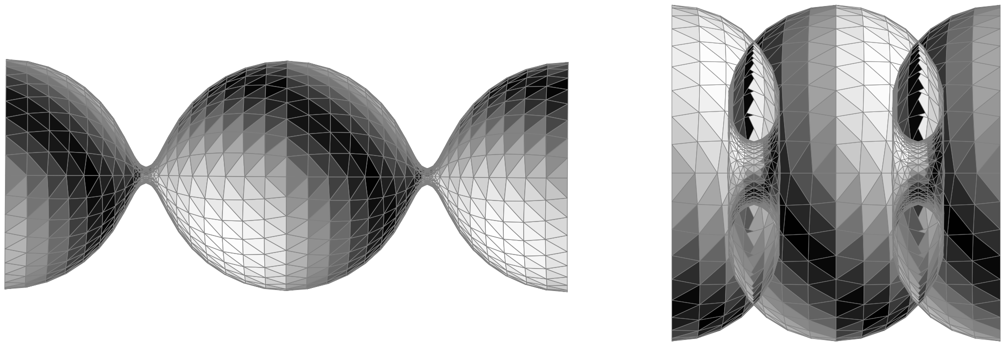

Figure 6: Delaunay surfaces: An embedded unduloid on the left, and on the right a nodoid cut open to display its self-intersections.

4 Candidates and necessary conditions

Basically we follow Kapouleas' recipe to obtain candidates of CMC surfaces. We start with a *graph* with almost, but not exactly, integer edge lengths. In the simplest case the edge length is always close to 2. Our CMC surfaces are close to spheres of radius 1 about the vertices of this graph. They are joined by handles whenever the respective vertices on the graph are joined by edges. Therefore the graph will be a topological retract of the CMC surface. However, unlike Kapouleas, we do not admit scalings of the graph. Instead, for a given graph we check for existence of the respective CMC surface. There are necessary conditions for the graph and the types of handles we can use that we want to describe in this section.

The prototypes of the handles we use are given by the Delaunay surfaces: We will construct *unduloidal handles* that look like those of the embedded unduloids, and, if small, resemble catenoids, and *nodoidal handles* that are close to the merely immersed nodoids (see Figure 6). Compared to a chain of spheres the period of the unduloids is bigger whereas the period of the nodoids is smaller. It is therefore reasonable to take unduloidal handles on the edges with length bigger than 2 and nodoidal handles on edges smaller than 2.

For the conjugate surface construction the type of handle we use is encoded in the data of the boundary polygon. A graph with planar symmetries and prescribed types of handles determines the vertex angles and total rotation of the boundary polygon, but not its lengths. In particular the two types of handles are distinguished by different values for the total turn of the normal τ_i. This can be seen for the Delaunay surfaces: On the meridian of an unduloid the interior normal has 0 total turn from one sphere to another, or almost $+\pi$ in a neighbourhood of a small neck; on the meridian of a nodoid the total turn is -2π between two spheres, or $-\pi$ in a neighbourhood of a small neck (cf. Figure 6). However different 'sizes' of the handles are not distinguished by a different turn of the normal but by a different weight, and therefore a different arc length, see the next subsection.

Kapouleas used these two types of handles. Other handles are possible, though: In [G-B1] n spheres are joined directly with each other. We believe these handles arise for compact CMC surfaces too, see Figure 12 and 13. In this case the graph contains edges with length close to 1, and the trinoidal handle is placed at the middle vertex .

4.1 The balancing formula

The balancing formula is due to Rob Kusner (see e.g. [KKMS, p.16ff]). To formulate the balancing formula we associate *weights* w_i to each edge (or handle) e_i of the underlying graph of a CMC surface. For each handle this weight is determined as the integral of the conormal of a homological 1-cycle minus the integral over the normal of a homological 2-cycle that is bounded by the 1-cycle. Suppose the surface has a symmetry plane across a handle. We can take the 1-cycle γ to be the planar curvature line in the symmetry plane winding once around a handle and bounding a disk D in the symmetry plane. Then $w_i = \text{length}(\gamma) - \text{area}(D)$.

For each vertex the balancing formula requires that weighted edges sum up to zero,

$$\sum w_i e_i = 0, \tag{7}$$

with the sum running over all edges emanating from the vertex. For a given graph we can check that the distribution of unduloidal and nodoidal handles (reflected in lengths bigger and less than 2) is consistent with the balancing formula, i.e. we consider the signs in (7) only. In particular, if all vectors e_i point into a half-space as they do on the outermost vertices of a compact CMC surface, then there must be both positive and negative weights, or unduloidal and nodoidal handles. The precise weights are assigned to the edges by the numerical algorithm for a surface with zero periods. Hence (7) can be viewed as a necessary condition for the periods to close.

4.2 Stability

Stability imposes limits on the 'size' of a fundamental domain we can deal with: Since we use (both theoretically and numerically) area minimizers to span a given spherical contour, we require that the spherical minimal patch M is *stable* with respect to a fixed boundary. This means that the second variation of area of M in S^3 is non-negative, or

$$0 \leq \delta^2_{uN}\text{area}(M) = \int_M |\nabla u|^2 - \left(2 + |A|^2\right) u^2 \tag{8}$$

holds for all compactly supported u (see e.g. [S]). On the other hand a CMC surface is a critical point of the functional area $-$ Hvol. It is called *stable* if the second variation of this functional is non-negative, or

$$0 \leq \delta^2_{uN}(\text{area}(\tilde{M}) - H\text{vol}(\tilde{M})) = \int_{\tilde{M}} |\nabla u|^2 - |\tilde{A}|^2 u^2, \tag{9}$$

see e.g. [BdC, L.2.8]. Provided the boundaries are fixed the stability of the euclidean CMC surface is equivalent to the stability of the conjugate minimal surface, that is: conjugation respects stability. We thank Rob Kusner who suggested the following lemma.

Lemma 4 *Suppose $M \subset \mathrm{S}^3$ is a simply connected minimal surface and $\tilde{M} \subset \mathbb{R}^3$ is its conjugate CMC surface. Then M is stable if and only if its conjugate $\tilde{M}$ is stable.*

Proof: We compare (8) and (9). If $A = \begin{pmatrix} \lambda & \kappa \\ \kappa & -\lambda \end{pmatrix}$ then $|A|^2 = 2\lambda^2 + 2\kappa^2$. As in (4) we get for a conformal metric $\tilde{A} = \begin{pmatrix} 1-\kappa & \lambda \\ \lambda & 1+\kappa \end{pmatrix}$ and therefore $|\tilde{A}|^2 = 2 + 2\lambda^2 + 2\kappa^2 = 2 + |A|^2$. $\square$

We remark that the our stability condition on the CMC surface is weaker than the physically expected one: We fix the boundary values ($u|_{\partial M} = 0$) rather than requiring the free boundary condition that the planar boundary curve can vary in the symmetry plane. On the other hand if CMC surfaces are considered as critical points for the area under a volume constraint then our condition is stronger: We require (9) for all u and not only for the volume preserving functions with $\int_M u = 0$.

It is useful to consider the fundamental patch in the degenerate situation of handle size 0, that for a collection of spheres. Clearly after reflection of this *degenerate CMC patch* periods will remain – this is because we started with a configuration of spheres that do not match exactly. The degenerate patch consists of a union of spherical triangles and two-gons. Since each nodoidal or unduloidal handle curve of the degenerate CMC patch has 0 length, the same holds on the boundary curve of the conjugate degenerate spherical patch. It is therefore a polygon having less edges and usually with self-intersections.

Our examples of CMC surfaces are close to spheres and stability persists over small deformations. Therefore it only makes sense to consider examples such that all the degenerate spherical patches are stable; in particular no two-gon should be bigger than a hemisphere.

5 The examples and their numerics

To show how the conjugate surface method applies to compact surfaces we computed three examples. We explain the Penta surface of genus 5 in detail and will be more sketchy with the genus 12 and 3 surfaces.

The genus 5 surface Penta consists of 6 bubbles in fivefold symmetry, see Figure 1. Its graph looks like a Chrysler star. Suppose the radial edges have length slightly less than 2. Then the six unit spheres of the initial surface relate as follows: Each outer sphere intersects the centre sphere, but the outer spheres leave some space in between each other. Accordingly we place positive weights, i.e. un-

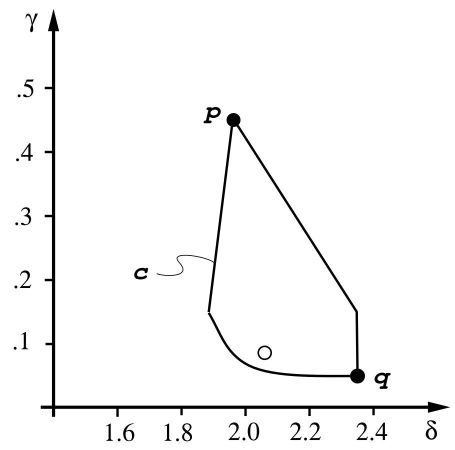

Figure 7: Numerical solution to the period problem for the Penta surface. The curve c with winding number 1 contains the solution with zero periods (at the empty circle) in its interior. The curve is plotted in terms of the lengths of two curves of the closed boundary polygon, see the table above. The fundamental patch displaying the periods at the points p and q is given in Figure 8.

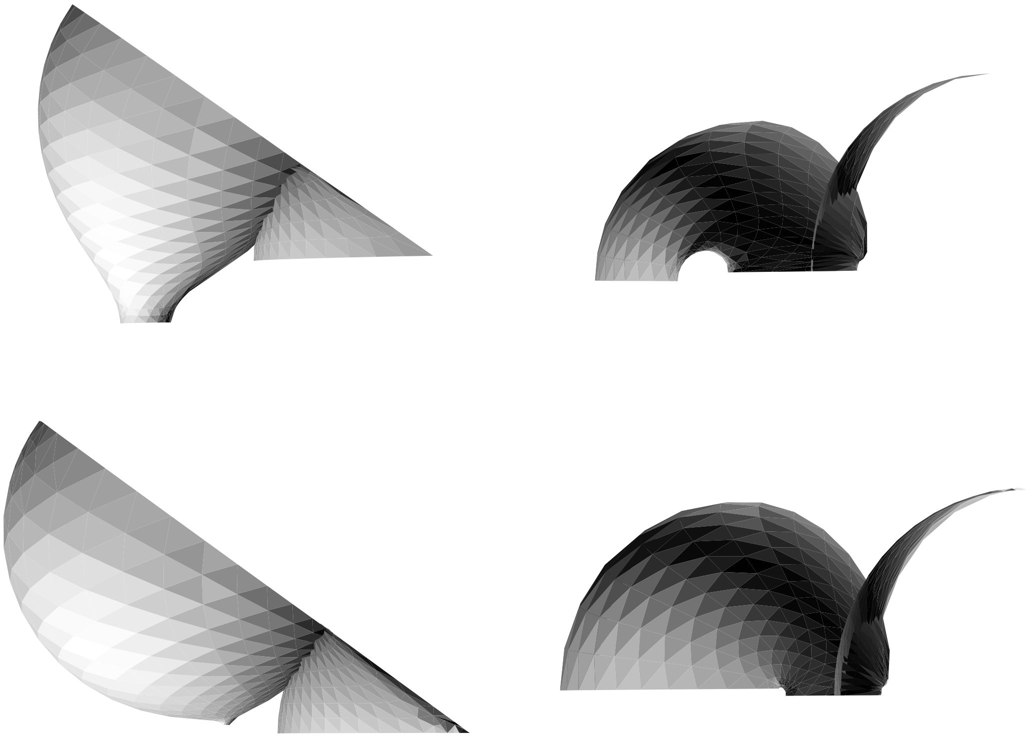

Figure 8: Fundamental domains of two Penta surfaces with non-vanishing periods. Top: Two different projections of the same fundamental domain at the point p on the curve c, see Figure 7. The two different periods are given by the distance between the pairs of horizontal boundary lines in each projection. Bottom: Same for fundamental domain at q. At this point both periods have the other sign compared to p.

duloidal handles, on the pentagonal edges, and negative weights, i.e. nodoidal handles, on the spokes. For appropriate 'sizes' or weights the balancing formula will be satisfied. The degenerate patch consists of a spherical triangle with edge lengths $\pi/5$, $\pi/2$, $\pi/2$ and a two-gon with angle $\pi/2$. Clearly these two spherical patches are stable.

In the following table we summarize the data for the surface. The second row is the unduloidal handle curve, the last row the long curve containing the nodoidal meridian.

arc (see Fig.7)	total turn of normal τ_i	edge angle at end of arc	length in degenerate patch	length of patch with closed periods
δ	$-\pi/5$	$\pi/2$	2.09	2.05
γ	$-\pi$	$\pi/2$	0	0.08
	π	$\pi/2$	1.67	1.72
	$-\pi/2$	$\pi/5$	1.57	1.63
	$-5\pi/2$	$\pi/2$	4.71	4.67

The periods give rise to a map f from the two-dimensional module space of the Penta surface (with non-closed periods) into the two-dimensional space of periods. To locally parameterize the Penta surfaces we choose two lengths of the boundary polygon, namely those of γ and δ in the table given above. We found a closed curve c in the module space displayed in Figure 7 whose image under f has winding number 1 around the origin in the period plane. The curve c must enclose a surface with zero period which occurs at the parameter values corresponding to the empty circle in Figure 7. More specifically, on each of the four arcs on c one period changes sign whereas the other period keeps its sign. Numerically, we computed the surfaces corresponding to the curve c. As an example we give the fundamental patch for two points p, q on c in Figure 8.

For the genus 12 surface the balanced graph is a dodecahedron with one extra vertex in the midpoint and 12 more edges joining the midpoint to the vertices. Take these edges of length slightly less than 2 and consider unit spheres about each vertex as a starting surface. Then the centre sphere intersects the 12 outer spheres, but these spheres do not touch each other. This is obvious from the fact that in the less symmetric regular sphere packing each sphere touches 12 spheres. Hence in the most symmetric packing some space must be left in between the spheres. Accordingly we take nodoidal handles on the radial edges and unduloidal handles on the dodecahedral edges. This surface was suggested by U. Abresch and is depicted in Figure 9.

The degenerate patch has two connected pieces: A spherical two-gon with angle $\pi/5$ (compare left hand side of Figure 10) and a spherical triangle with angles $\pi/2$, $\pi/5$, $\pi/3$ that is fundamental on S^2 for the symmetry group of the dodecahedron (see right hand side of the same figure). Again we summarize the data in a table. The table runs through the arcs in the anti-clockwise sense starting at the top left arc on Figure 10 or 11. The data in column 1 and 3 can be computed using trigonometric formulas.

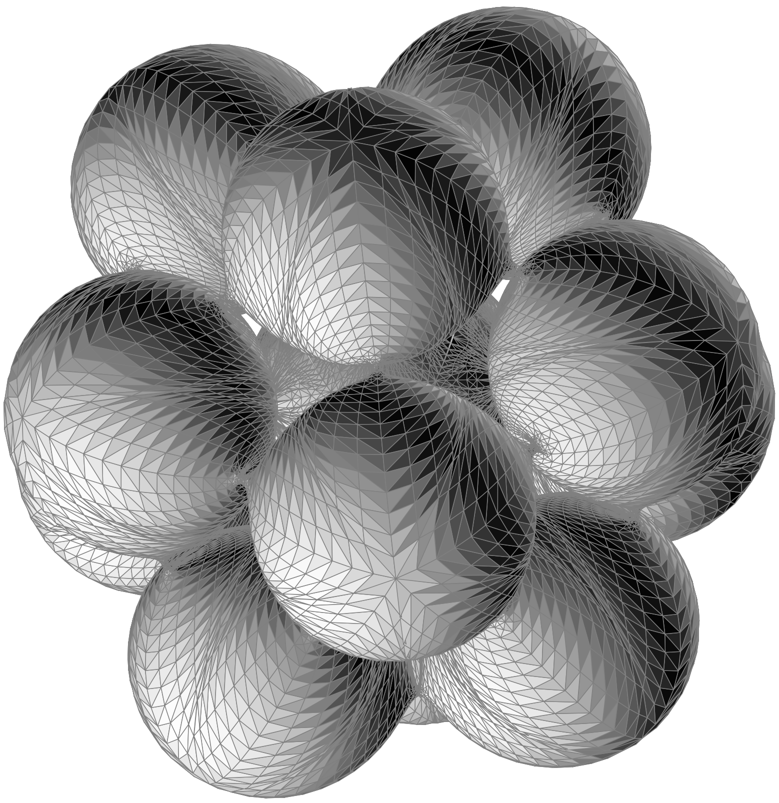

Figure 9: Surface of genus 12 with the symmetry of a dodecahedron with unduloidal handles between the outer spheres and nodoidal handles joining each outer sphere with the centre sphere.

total turn of normal τ_i	edge angle at end of arc	length in degenerate patch	length of patch with closed periods
-0.554	$\pi/2$	1.94	1.74
$-\pi$	$\pi/2$	0	0.10
$-\pi$	$\pi/2$	1.57	1.77
-0.365	$\pi/3$	0.55	0.36
-6.94	$\pi/5$	3.79	3.59

The underlying graph of the genus 3 surface is an equilateral triangle with three more edges from its midpoint to the triangle vertices. We take these spokes of length slightly bigger than 1. The degenerate surface consists of three spheres. These are joined by a trinoidal centre and nodoidal handles between each other. The numerical evidence for this surface is not conclusive: A small period remained, see Figure 14.

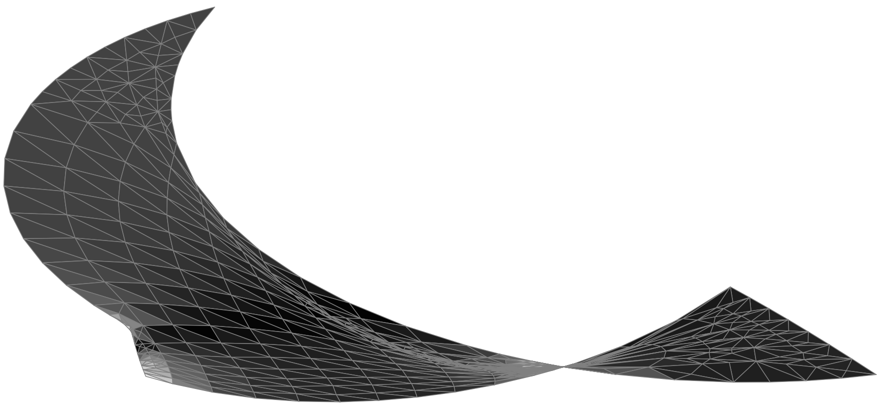

Figure 10: Fundamental domain for the dodecahedral surface stereographically projected from S^3 to $\mathbb{R}^3$. The small arc at the bottom left is the arc going half round the unduloidal handle, compare next figure. In the degenerate situation this arc has 0 length; the patch is then disconnected and conists of a two-gon with angle $\pi/5$ on the left and a spherical triangle on the right.

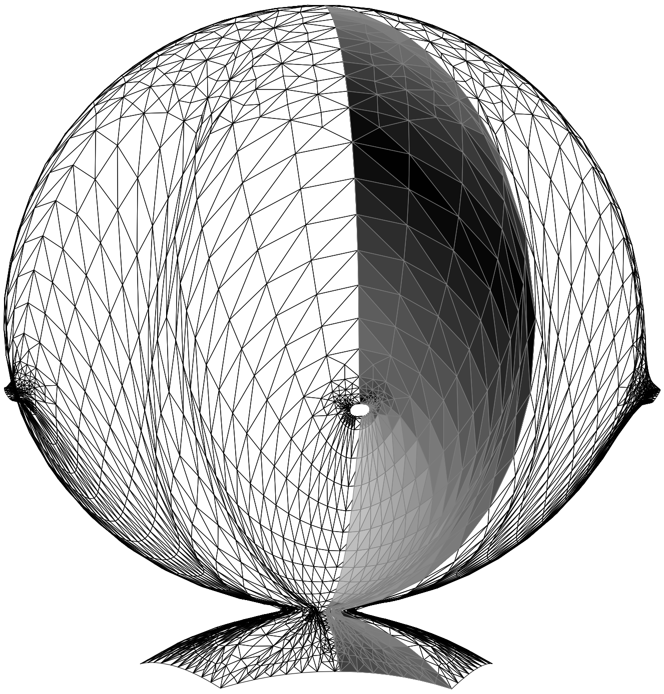

Figure 11: Dodecahedral surface: One of the 12 outer bubbles that are attached to the centre-sphere with a nodoidal handle. A fundamental domain, conjugate to the spherical patch depicted in Figure 10 is highlighted.

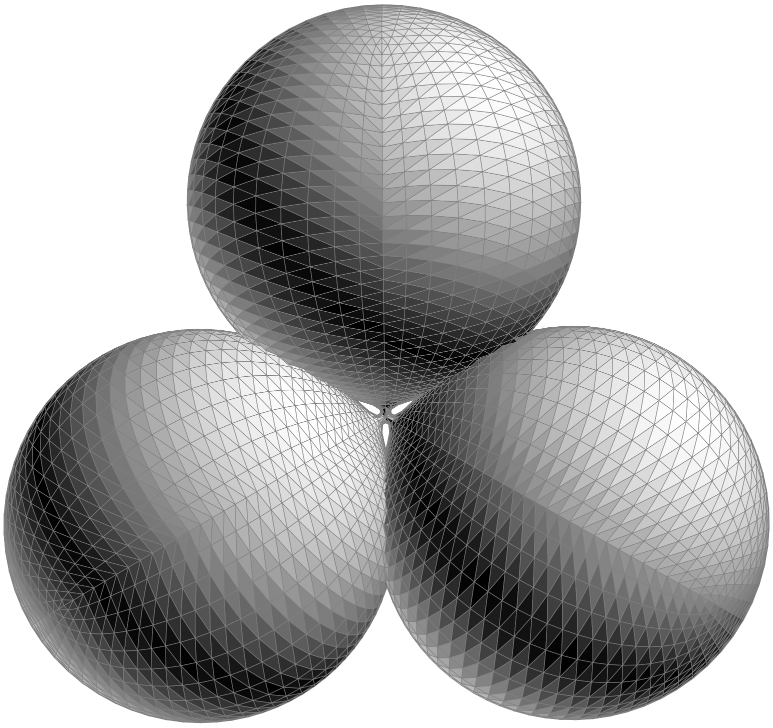

Figure 12: A genus 3 CMC surface. The existence of this surface is not settled, since we did not achieve a complete closure of the period, see Figure 14 and Section 5.

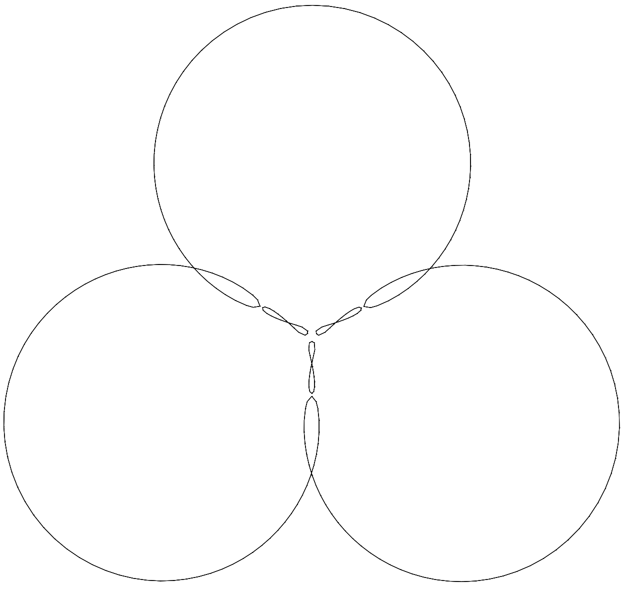

Figure 13: The intersection of the genus 3 surface with its symmetry plane displays the trinoidal handle in the centre and the nodoidal handles joining the bubbles pairwise.

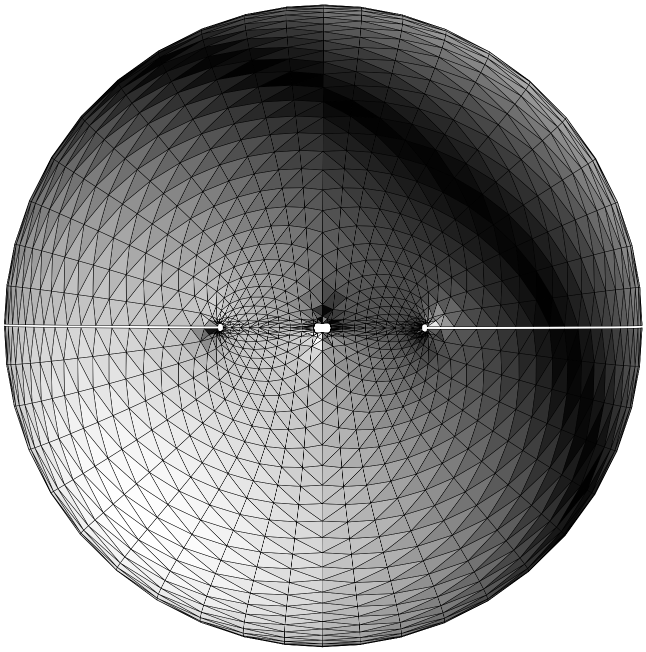

Figure 14: One bubble of the genus 3 CMC surface displays the remaining period.

References

[ADNS] Anderson, D.M., H.T. Davis, J.C.C. Nitsche, L.E. Scriven: Periodic surfaces of prescribed mean curvature Advances in chem. phys. **77**, New York: Wiley 1990

[BdC] J. Barbosa, M. do Carmo: Stability of hypersurfaces with constant mean curvature, Math. Zeit. **185**, 339-353 (1984).

[Bo] A.I. Bobenko: All constant mean curvature tori in R^3, S^3, H^3 in terms of theta functions, Math. Ann. **290**, 209-245 (1991)

[Br] K. Brakke: The surface evolver, Exp. Math. **2**, 141-165, 1992

[EKT] Ercolani, N., H. Knörrer, E. Trubowitz: Hyperelliptic curves that generate constant mean curvature tori in $\mathbb{R}^3$. The Verdier Memorial Conference on integrable systems, Actes du colloque international de Lumingy 1991.

[G-B1] K. Große-Brauckmann: New surfaces of constant mean curvature, Math. Zeit. **214**, 527-565 (1993)

[G-B2] K. Große-Brauckmann: A geometric existence proof for Wente-tori, preprint 1993

[H] M. Heil: PhD-thesis, TU Berlin, in preparation

[J] Jaggi, C.: On the classification of constant mean curvature tori in $\mathbb{R}^3$. Preprint ETH-Zürich, 1993.

[Ka] Karcher, H.: The triply periodic minimal surfaces of A. Schoen and their constant mean curvature companions. man. math. **64**, 291-357 (1989)

[Kp1] Kapouleas, N.: Compact constant mean curvature surfaces in Euclidean three-space. J. Diff. Geom. **33**, 683-715 (1991)

[Kp2] Kapouleas, N.: Constant mean curvature surfaces constructed by fusing Wente tori. preprint

[KKMS] Korevaar, N., R. Kusner, W.H. Meeks, B. Solomon: Constant mean curvature surfaces in hyperbolic space, Am. J. Math. **114**, 1-43, (1992)

[L] Lawson, H.B.: Complete minimal surfaces in S^3. Ann. of Math. **92**, 335-374 (1970)

[O] Oberknapp, B: Diplomarbeit Bonn, in preparation

[OP] Oberknapp, B, K. Polthier: A numerical algorithm for discrete surfaces with constant mean curvature, in preparation

[PP] Pinkall, U., Polthier, K.: Computing discrete minimal surfaces and their conjugates, Exp. Math. **2**, 15-36, 1993

[PS] Pinkall, U., Sterling, I.: On the classification of constant mean curvature tori. Ann. of Math. **130**, 407-451 (1989)

[S] Schoen, R.: Estimates for stable minimal surfaces in three dimensional manifolds. In: Seminar on Minimal Submanifolds, Ann. of math. stud. **103**. Princeton: 1983

[W] Wente, H.: Counterexample to a conjecture of H. Hopf, Pac.J. of Math. **121**, 193-243, 1986

Address of the authors
Technische Universität Berlin
FB 3 Mathematik, MA 8-3
Str. des 17. Juni 136
10623 Berlin
kgb@sfb288.math.tu-berlin.de
polthier@math.tu-berlin.de